Enhanced molecular alignment by short laser pulses

M. Leibscher,[1] I. Sh. Averbukh,[1] and H. Rabitz[2]
[1]*Department of Chemical Physics, The Weizmann Institute of Science, Rehovot 76100, Israel*
[2]*Department of Chemistry, Princeton University, Princeton, New Jersey 08544, USA*
(Received 1 August 2003; published 15 January 2004)

We study molecular alignment by trains of strong, ultrashort laser pulses. Single-pulse alignment is analyzed both in classical and quantum-mechanical regimes. Moreover, we suggest multipulse excitation schemes leading to dramatically enhanced molecular alignment, and define conditions for femtosecond experiments of this kind.

DOI: 10.1103/PhysRevA.69.013402 PACS number(s): 32.80.Lg, 33.80.−b, 02.30.Yy

I. INTRODUCTION

The ability to align or orient macroscopic samples of molecules is crucial for many applications in chemical reaction dynamics, surface processing, and ultrafast optics. Molecular alignment with the help of lasers has become an intensively studied subject in the last years (for a recent review see, e.g., Ref. [1]). Strong nonresonant laser fields have been shown to yield molecular alignment along the field polarization direction [2–5] by creating pendular molecular states [6–8]. By adiabatically turning on the laser field, the molecules may be trapped in pendular states the angular width of which reduces with increasing intensity of the laser. However, this molecular alignment disappears when the field is turned off adiabatically. On the other hand, rather short laser pulses may create rotational wave packets that take a noticeable aligned shape *after the end of the pulse* [9–21], even under thermal averaging [22,23]. Alternatively, free aligned rotational wave packets may be created by a sharp truncation of an adiabatic strong laser pulse [24,25]. Once being generated, aligned rotational states periodically retain the angularly squeezed shape because of the phenomenon of quantum revivals. Many applications may benefit from that transient alignment *at field-free conditions*. Generation of ultrashort light pulses [26,27] and control of high harmonics generation [28] are only a few examples to mention.

Recently, we showed that there is a limit to the degree of molecular alignment that can be attained by a single, ultrashort laser pulse [29]. In order to achieve enhanced field-free molecular alignment beyond this limit, more complex pulse shapes should be used. Methods of optimal control have been applied to this problem in the past, providing rather sophisticated field patterns [30–34]. A novel strategy for producing angularly squeezed states of a rigid rotor by a specially tailored series of short laser pulses was suggested in Ref. [35]. The proposed ''accumulative squeezing'' scheme leads to a dramatic narrowing of the rotor angular distribution upon increasing the number of the pulses. An atom optics realization of this strategy [36] has been already experimentally demonstrated [37]. Enhanced molecular alignment by trains of ultrashort laser pulses seems to be a feasible experimental procedure as well [29,35,38].

In a recent study [29], we proposed optimal two- and three-pulse schemes for effective field-free molecular alignment. In the present work, we investigate the single- and multipulse alignment of molecules in the classical and quantum-mechanical regime in more detail. We analyze and compare several strategies for enhanced multipulse molecular alignment. With help of quantum control theory, we define parameters for optimal molecular alignment under various conditions, including different temperature regimes. The paper is organized as follows. Section II describes Hamiltonian of the system, and presents the action of a short pulsed kick on a three-dimensional quantum rigid rotor. Section III analyzes the time-dependent alignment factor (measure of the angular distribution width) following a single short pulse, both in the quantum and classical limits. Optimal molecular alignment with a train of pulses is studied in Sec. IV for various pulse types. The results are summarized in Sec. V. The paper also contains two Appendixes with the details of the calculations.

II. THREE-DIMENSIONAL KICKED ROTOR

Under certain conditions, the process of molecular alignment by laser fields can be described by a strongly driven three-dimensional (3D) rigid-rotor model. The Hamiltonian of a three-dimensional driven rotor is

$$H=\frac{\vec{L}^2}{2I}+V(\theta,t), \tag{1}$$

where L is the angular momentum of the rotor, I is its moment of inertia, and θ is the angle between the field polarization and molecular axis. A linear molecule without a permanent dipole couples to the external field via induced polarization. For nonresonant laser fields, this interaction, averaged over fast optical oscillations, is (see, e.g., Ref. [39])

$$V(\theta,t)=-\tfrac{1}{4}\mathcal{E}^2(t)[(\alpha_{\parallel}-\alpha_{\perp})\cos^2(\theta)+\alpha_{\perp}]. \tag{2}$$

Here $\alpha_{\parallel}$ and $\alpha_{\perp}$ are the components of the polarizability, parallel and perpendicular to the molecular axis, and $\mathcal{E}(t)$ is the *envelope* of the laser pulse. By introducing the dimensionless time $\tau=t\hbar/I$ and the interaction strength $\epsilon=(\alpha_{\parallel}-\alpha_{\perp})\mathcal{E}^2(t)I/(4\hbar^2)$, the Hamiltonian can be written as

$$H=\frac{\vec{L}^2}{2}-\epsilon(\tau)\cos^2\theta. \tag{3}$$

 ©2004 The American Physical Society

We assume that the rotor is initially in its ground state, $\psi(\theta,0)=Y_0^0(\theta)$. The wave function of the system can be expanded in spherical harmonics, the eigenfunctions of the free 3D rotor,

$$\psi(\theta,\tau)=\sum_{l=0}^{\infty} a_l(\tau)Y_l^0(\theta). \tag{4}$$

Since the interaction with the laser field depends only on $\cos\theta$, the z component of the angular momentum is conserved during the interaction. In order to obtain the coefficients $a_l(\tau)$ for any time dependence of $\epsilon(\tau)$ we numerically integrate the Schrödinger equation with the Hamiltonian in Eq. (3). If the interaction with the field is short compared to the typical rotational period of the rotor (δ kick), the wave function after the interaction can be expressed as

$$\psi(\theta,0^+)=\exp(iP\cos^2\theta)\psi(\theta,0^-), \tag{5}$$

where $P=\int\epsilon(\tau)d\tau$ is the dimensionless interaction strength. The wave function at time τ after the pulse is

$$\psi(\theta,\tau)=\frac{1}{\sqrt{4\pi}}\sum_{l=0}^{\infty} c_l\exp[-il(2l+1)\tau]Y_{2l}^0(\theta), \tag{6}$$

where $\tau=t\hbar/I$ is the dimensionless time. The coefficients c_l are given by

$$c_l=\sqrt{\pi(4l+1)}(iP)^l\frac{\Gamma\left(l+\frac{1}{2}\right)}{\Gamma\left(2l+\frac{3}{2}\right)}{}_1F_1\left(l+\frac{1}{2},2l+\frac{3}{2},iP\right). \tag{7}$$

where ${}_1F_1$ is the confluent hypergeometric function. Equation (7) is obtained by expanding $\exp(iP\cos^2\theta)$ in terms of spherical harmonics (see Appendix A).

III. ALIGNMENT AFTER A SINGLE PULSE

In the following, we study the alignment of a molecular system subject to a single (short) pulse, considering a system that is initially in its ground state (zero temperature). We use the alignment factor $A(\tau)=\langle 1-\cos^2\theta\rangle$ to characterize quantitatively the degree of molecular alignment. Defined in this way, the alignment factor coincides with the variance of θ for well-aligned molecules ($\theta\ll 1$) and becomes zero if the alignment is perfect.

We start with analyzing a classical ensemble of rotors, or equivalently, an ensemble of particles moving on a sphere. Classically, a rigid rotor driven by the external field, Eq. (2), gains the angular velocity

$$\omega=-P\sin(2\theta_0) \tag{8}$$

as a result of a δ kick, where θ_0 is the initial angle of the rotor. After the kick, the rotor evolves freely, so that

$$\theta(\tau)=\theta_0-P\tau\sin(2\theta_0). \tag{9}$$

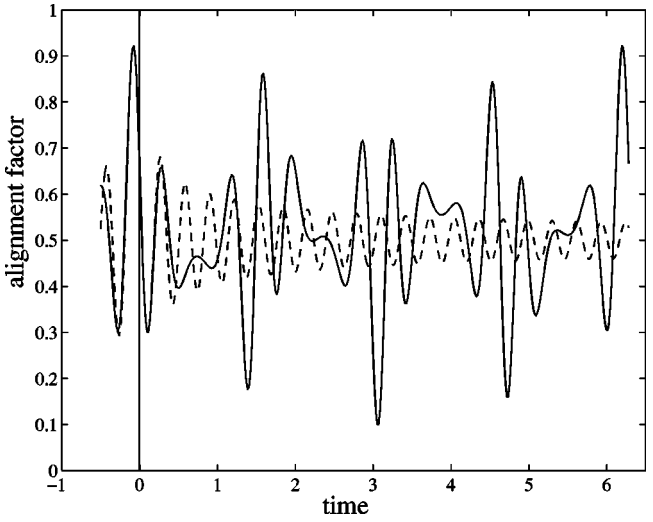

FIG. 1. Quantum-mechanical (solid line) and classical (dashed line) alignment factor for kick strength $P=10$.

If the initial angular velocity of all rotors of the ensemble is zero, the classical alignment factor can be calculated by averaging over the isotropic initial angular distribution, that is,

$$A_{cl}(\tau)=1-\frac{1}{2}\int_0^{\pi} d\theta_0\sin\theta_0\cos^2[\theta_0-P\tau\sin(2\theta_0)]. \tag{10}$$

The classical alignment factor can be expressed in terms of hypergeometric functions (see Appendix B):

$$A_{cl}(\tau)=\frac{1}{2}+\frac{1}{6}{}_1F_2\left(1;\frac{7}{4},\frac{5}{4};-(P\tau)^2\right)-\frac{8}{15}\tau{}_1F_2\left(2;\frac{7}{4},\frac{9}{4};-(P\tau)^2\right). \tag{11}$$

We note that the dynamics of a classical rotor depends only on the product $P\tau$. The kick strength defines the time scale of the process, but does not affect the shape of the $A_{cl}(\tau)$ graph. The dashed line in Fig. 1 shows the classical alignment factor as a function of time. Starting from a uniform distribution $[A_{cl}(0)=2/3]$, the particles in the northern hemisphere start moving towards the north pole ($\theta=0$), and the particles in the southern hemisphere move towards the south pole ($\theta=\pi$). For a pictorial representation of the time-dependent angular distribution of a kicked 3D classical rotor and the discussion of related semiclassical catastrophes in the distribution (focusing, rainbows, glory) see Refs. [38,40]. The point of maximal angular squeezing (minimal value of the alignment factor) is reached when most of the particles are concentrated in the vicinity of the poles ($A_{min}\approx 0.30$ at $\tau\approx 0.1$ after the kick). The classical alignment factor oscillates around the value $A_{cl}(\tau\to\infty)=1/2$.

In the quantum-mechanical description, the alignment factor can be expressed as

$$A(\tau)=1-M-\frac{1}{2\pi}\mathrm{Re}\sum_{l=0}^{\infty} c_l c_{l+1}^{*} \times\exp[i(4l+3)\tau] \times\frac{(2l+1)(2l+2)}{4l+3}\frac{1}{\sqrt{(4l+1)(4l+5)}}, \quad (12)$$

with

$$M=\frac{1}{4\pi}\sum_{l=0}^{\infty}|c_l|^2\frac{1}{4l+1}\left[\frac{(2l+1)^2}{4l+3}+\frac{4l^2}{4l-1}\right]. \quad (13)$$

Note that the coefficients c_l [see Eq. (7)] depend on the kick strength P. Here, M is the time-averaged value of $\langle\cos^2\theta\rangle$. The solid line in Fig. 1 shows the quantum-mechanical alignment factor for the kick strength $P=10$. We see that the classical and quantum-mechanical alignment factors coincide for $\tau\ll 1$, which means that shortly after the kick, the system behaves more or less classically. However, the dynamics of a quantum-mechanical rigid rotor is completely periodic, and the alignment factor repeats itself after one revival period, $T_{rev}=2\pi$. Moreover, we can see minima of the alignment factor at $\tau\approx\pi/2$ and $\tau\approx\pi$, which do not appear in the classical picture. The global minimum of the alignment factor ($A_{min}\approx 0.097$, which is roughly one-third of the classical value) occurs in the quantum domain at $\tau\approx 3.06$ after the kick. Although the appearance of the global minimum at $\tau\approx\pi$ is a purely quantum-mechanical phenomenon, we can relate this minimal alignment factor to a classically defined value. For this, we consider the alignment factor for *negative times* (which corresponds to kicking the system to the equator direction). In Fig. 1 one can see a maximum of the alignment factor for small negative times, where the system still behaves classically ($A_{max}\approx 0.925$ at $\tau\approx -0.08$). The periodicity of the quantum-mechanical alignment factor allows us to relate this value to the corresponding value at $\tau\approx\pi$. It follows from Eq. (12) that

$$A(\pi+\Delta\tau)=1-A(\Delta\tau)+(1-2M), \quad (14)$$

where M is given by Eq. (13). We expect M to be equal to 1/2 in the classical limit, when all the kicked particles rotate uniformly along the circular trajectories passing through the poles. Figure 2(b) shows M as a function of the kick strength P. As can be seen, it is always smaller than 1/2 and approaches this value for $P\to\infty$. It means that for large enough values of P we may neglect the term $(1-2M)$ in Eq. (14), and the globally minimal quantum alignment factor can be estimated via the "classical" maximal value A_{max} as $A(\tau)=1-A_{max}=0.075$. The global minimum of the alignment factor near $\tau\approx\pi$ depends in a nonmonotonic way on the kick strength. As can be seen in Fig. 2(a), there are "magic" kick-strength values that provide local minima of the alignment factor as a function of P ($P_{m1}=5.4, P_{m2}=11.8, P_{m3}=18.2,\ldots$). It is worth mentioning that our analytical results are in very good agreement (both qualitative and quantitative) with recent direct numerical simulations [23] of postpulse alignment of a NaI molecule excited by a very short off-resonant strong laser pulse (compare Figs. 1 and 2 of the present paper with Figs. 1 and 4 from Ref. [23]).

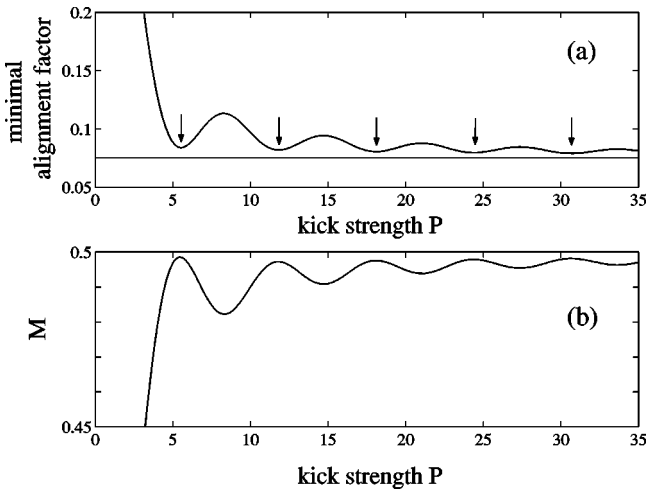

FIG. 2. The minimal alignment factor plotted as a function of the kick strength P (a). The line indicates the classical value and the arrows mark the "magic" kick strengths. The P dependence of the factor M, Eq. (13), is shown in (b).

Single-pulse alignment at finite temperature

Next, we study the effect of a finite initial temperature on the molecular alignment by short pulses. If the temperature of the system is nonzero, the alignment factor has to be averaged over the all contributing initial states, so that

$$A(\tau)=\sum_{l_0=0}^{\infty}P(l_0)\sum_{m_0=-l_0}^{l_0}A_{l_0}^{m_0}(\tau), \quad (15)$$

where

$$P(l_0)=\frac{1}{Q}\exp\left[-\frac{l_0(l_0+1)}{2\sigma_{th}^2}\right] \quad (16)$$

is the thermal distribution at temperature T, with $\sigma_{th}=(k_BT/2B)^{1/2}$. Here, k_B is the Boltzmann constant, Q is the partition function, $B=\hbar^2/2I$ is the rotational constant, and

$$A_{l_0}^{m_0}(\tau)=1-\langle\psi(\tau)|\cos^2\theta|\psi(\tau)\rangle \quad (17)$$

is the alignment factor for the initial state $|l_0,m_0\rangle$. Since the quantum number m is preserved during the interaction, we can write

$$|\psi(\tau)\rangle=\sum_{l=0}^{\infty}a_l^{m_0}(\tau)\exp\left[-\frac{i}{2}l(l+1)\tau\right]|l,m_0\rangle. \quad (18)$$

For an arbitrary time dependence of the pulse, the coefficients $a_l^{m_0}(\tau)$ can be obtained by numerically integrating the Schrödinger equation. For the case of a δ-kicked rotor, the problem has an analytical solution,

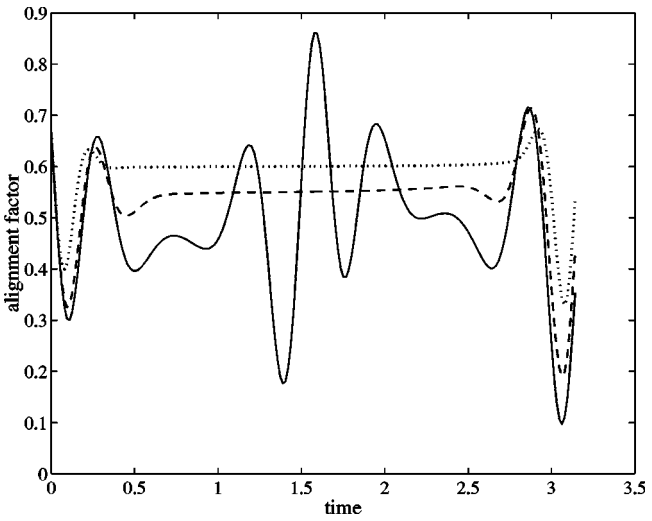

FIG. 3. Quantum-mechanical alignment factor for kick strength $P=10$. The solid line represents the alignment factor at zero temperature. For the dashed (dotted) line, the temperature T corresponds to $\sigma_{th}=1.74$ and $\sigma_{th}=3.9$, respectively.

$$a_l^{m_0}(\tau)=a_l^{m_0}=\sum_{l'=0}^{\infty} c_{l'}\sqrt{\frac{(2l'+1)(2l_0+1)}{2l+1}} \times\langle l',l_0,0,0|l,0\rangle\langle l',l_0,0,m_0|l,m_0\rangle, \tag{19}$$

where c_l is given in Eq. (7). With the help of Eq. (18), we can write

$$A_{l_0}^{m_0}(\tau)=1-\sum_{l=0}^{\infty}\alpha_l^{m_0}|a_l^{m_0}(\tau)|^2 -2\,\mathrm{Re}\sum_{l=0}^{\infty}\beta_l^{m_0}a_{l+2}^{m_0}(\tau)a_l^{m_0*}(\tau)\exp[-i(2l+3)\tau], \tag{20}$$

where

$$\alpha_l^{m_0}=\frac{1}{2l+1}\left[\frac{(l+1)^2-m_0^2}{2l+3}+\frac{l^2-m_0^2}{2l-1}\right] \tag{21}$$

and

$$\beta_l^{m_0}=\frac{1}{2l+3}\sqrt{\frac{[(l+1)^2-m_0^2][(l+2)^2-m_0^2]}{(2l+1)(2l+5)}}. \tag{22}$$

Figure 3 shows the averaged alignment factor for different temperatures compared to the zero-temperature case (solid line). For $\sigma_{th}=1.74$ (dashed line) and $\sigma_{th}=3.9$ (dotted line), the oscillations around $\tau=\pi/2$ are completely washed out. However, the pronounced minima around $\tau=0$ and $\tau=\pi$ are preserved. For ICl molecules that have rotational constant of $B=0.114\ \mathrm{cm}^{-1}$ and polarizability anisotropy $\Delta\alpha=\alpha_{\parallel}-\alpha_{\perp}=9A^3$ [41], $\sigma_{th}=1.74$ corresponds to temperature $T=1$ K, and $\sigma_{th}=3.9$ corresponds to $T=5$ K.

IV. OPTIMAL ALIGNMENT WITH SEVERAL PULSES

Until now, we only considered the interaction of the molecular system with a single short laser pulse. However, the molecular alignment can be improved by applying a series of several laser pulses. A regular strategy to enhance the alignment (or orientation) of a kicked rotational system was proposed in Ref. [35]. As mentioned above, the angular distribution of the molecules is maximally squeezed at some time $\Delta\tau_1$ after the first kick. According to the ''accumulative squeezing strategy'' [35], the second kick is applied exactly at that time, $\tau_2=\Delta\tau_1$. Immediately after the second kick, the system has the same angular distribution as before the kick, but $\tau=\tau_1$ is no longer a stationary point for the alignment factor $A(\tau)$. As a result, $A(\tau)$ will reach a new minimal value at some point $\tau_2+\Delta\tau_2$, and this new minimum will be smaller than the previous one. By continuing this way, one can apply a sequence of kicks at time instants $\tau_{k+1}=\tau_k+\Delta_k$, and the amount of alignment will accumulate with time.

Although this strategy leads, in principle, to an unlimited alignment by applying more and more pulses, it can be made even more efficient by a proper optimization, especially if only a few pulses are used. The problem of coherent and optimal laser control of rotational degrees of freedom has been already addressed in several publications [30–34,36]. Here we specifically analyze the optimal routes to molecular alignment by a series of short laser pulses by minimizing the alignment factor with respect to a certain number of parameters describing the shape of the pulses. This class of optimal fields is especially attractive for potential experimental realization of the enhanced angular squeezing.

Assuming that the shape of the laser pulses is Gaussian, the time-dependent interaction strength in Eq. (3) can be written as

$$\epsilon(\tau)=\sum_{j=1}^{N}P_j'\exp\left(-\frac{(\tau-\tau_j)^2}{\sigma^2}\right), \tag{23}$$

where P_j' are the peak intensities, and σ is the duration of N pulses. The delay times between the pulses are denoted by τ_j. In order to find the optimal sequence of N pulses, we numerically solve the Schrödinger equation with the Hamiltonian of Eq. (3) and minimize the alignment factor. Due to nonlinearity, the optimization problem is rather involved even for $N=2$ or 3. Therefore, we first reduce the number of parameters by imposing various restrictions on the shape of the pulses. These restrictions are then gradually removed, using the previous results as the starting point for more complex optimization schemes. In the following, we summarize the results of the different optimization problems. In Secs. A–C, we assume that the molecular system is initially in its ground state. The effect of finite initial temperature is discussed in Sec. D.

A. Alignment with identical δ kicks

First, we consider only very short pulses, so that the Gaussian pulse shape in Eq. (23) is reduced to a δ function

TABLE I. Accumulative and optimal alignment with identical pulses in the classical regime.

No.	A_{acc}	A_{opt}
1	0.297	0.297
2	0.219	0.215
3	0.169	0.137
4	0.137	0.086

with the strength $P_j = P'_j \sigma\sqrt{\pi}$. Moreover, we assume that all pulses have the same strength $P_j = P$. As the first step, we will treat the problem classically. In this case, the number of parameters is reduced even more because, as it can be seen from Eq. (10), the optimal classical alignment factor does not depend on the kick strength. The latter defines only the time scale of the driven rotational dynamics. The only relevant parameters are the (normalized) delay times between the kicks. Table I compares the best alignment for up to four pulses applied according to the accumulative squeezing strategy [35] and for the optimal sequence of pulses. It can be seen that for two pulses, the optimal solution is only slightly better than the accumulative squeezing. However, for three and four pulses a considerable improvement can be achieved by optimizing the delay times between the pulses.

In the quantum-mechanical regime, the alignment factor does depend on the kick strength P. Therefore, we have to perform the optimization for different values of P. The results of the quantum optimization for two δ kicks can be seen in Fig. 4. Here we looked for a pulse sequence in which the second pulse is applied with a short delay ($\tau_1 \ll T_{rev} = 2\pi$) after the first pulse, using the results of the classical optimization as the starting guess. The figure shows the minimal alignment factor as a function of P. We can see that for $P > 4$, the alignment factor is almost independent of P and has the classical value $A_{min} \approx 0.21$ (see Table I). However,

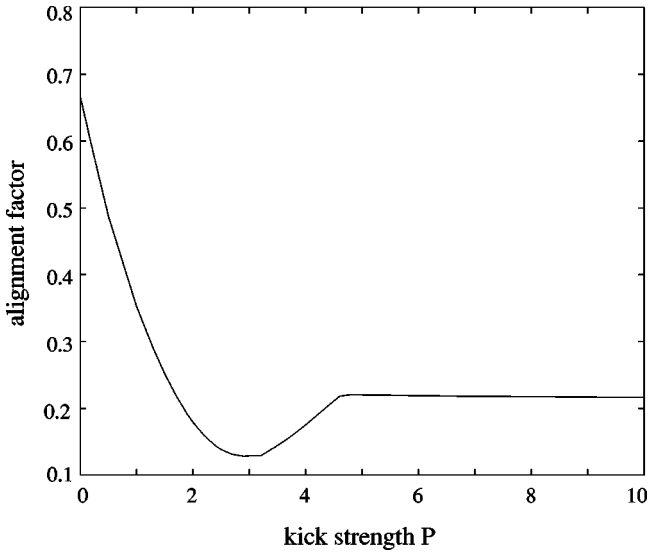

FIG. 4. Minimal alignment factor for a system kicked with two pulses, where the second pulse is applied in the vicinity of the first pulse, as a function of the kick strength P.

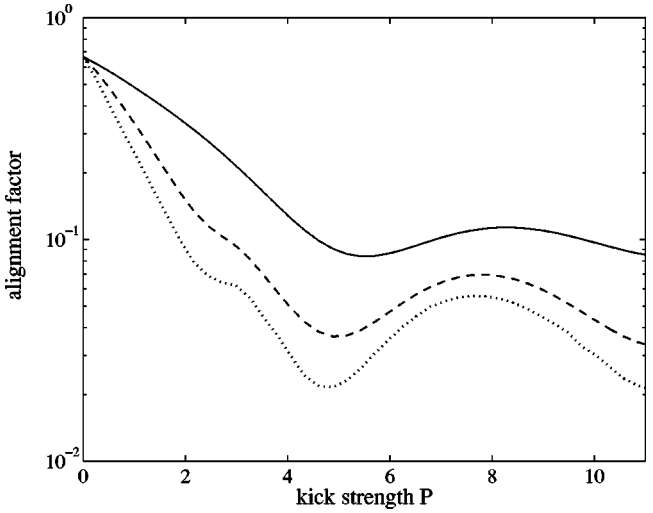

FIG. 5. Minimal alignment factor as a function of the kick strength P for a system kicked by one pulse (solid line) and for the optimized sequence of two (dashed) and three (dotted line) identical pulses.

for $P < 4$ we observe a strong dependence on P and find the best value for the alignment factor $A_{min} \approx 0.13$ for $P \approx 3$, which is almost half of the ''classical'' value. We note that the same behavior, which is of purely quantum-mechanical origin, was observed in a related problem of squeezing cold atoms by pulsed optical lattices [36]. The previous results permit finding the local quantum optimum for the alignment problem in the vicinity of the classical solution. However, the most profound alignment of a molecular system kicked by a single δ pulse occurs deeply in the quantum domain, around $\tau = T_{rev}/2 = \pi$ (see Fig. 1). Therefore, it can be assumed that a second pulse with a delay time $\tau_1 \approx \pi$ leads to a more effective alignment. The optimization results corresponding to this initial guess are indeed better, as shown in Fig. 5. The three curves present the minimal value of the alignment factor for one, two, and three pulses as a function of the kick strength P. We searched for the optimal solution for in case when the second pulse is applied around $\tau_2 = \pi$ after the first pulse, and the third pulse acts shortly after the second one. Shifting the third pulse again by $\tau_3 \approx \pi$ does not result in further improvement of the alignment. We see that the quality of alignment can be considerably improved by applying two or three pulses instead of one. The P dependence of the alignment factor shows nonmonotonous behavior also for two and three kicks. The first minimum occurs at $P = 4.88$. For $N = 2$, it is $A_{min} = 0.037$ and for $N = 3$, the minimal value $A_{min} = 0.022$ can be achieved. With three equal pulses, the alignment can be improved by almost a factor of 4 compared to the results achieved with a single kick of an arbitrary strength.

B. Alignment with δ kicks of different strength

Another possibility to further improve the angular squeezing is to use pulses with different strength. We start with proposing a simple, but effective two-pulse excitation scheme. The first pulse prealigns the molecules and concen-

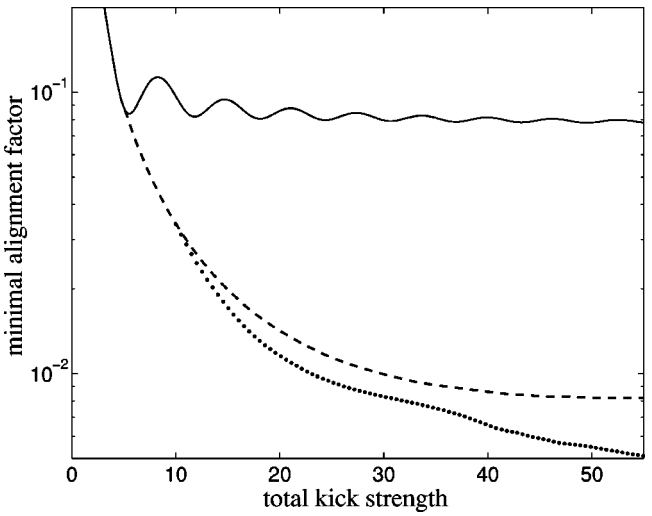

FIG. 6. Optimal alignment factor of a 3D rotor kicked with a single pulse (solid line), or with a sequence of two (dashed line) or three (dotted line) pulses for the given total kick strength P_t.

trates them in the harmonic region of the angular interaction potential. In order to estimate the efficiency of the process, we choose the first magic kick strength $P_{m1}=5.4$ for the first pulse. The second pulse is applied at the time of minimal angular spread (delay time $\tau_1=2.99$). It should be much stronger than the first pulse, so that the kinetic energy gained by the molecules during the first kick can be neglected. In this limit, the second pulse provides a classical-like alignment of the ''frozen'' angular distribution formed by the first pulse in the harmonic region. For $P_2 \geqslant 50$, the minimal alignment factor $A_{min}=0.017$ can be achieved. This way, the degree of molecular alignment can be improved by more than a factor of 4 compared to the single-pulse alignment. Further improvement of molecular alignment could be achieved by continuing this procedure with three and more pulses.

In order to explore the prospects of multikick alignment more systematically, we minimize the alignment factor keeping the total kick strength $P_t=\Sigma_{j=1}^{N} P_j$ fixed. The result of the optimization is shown in Fig. 6. Here, the minimal alignment factor for $N=1$ (solid line), $N=2$ (dashed line), and $N=3$ (dashed dotted line) pulses is plotted as a function of P_t. Exemplary excitation parameters are shown in Table II. For small total kick strength $P_t<5$, single-pulse and multipulse excitations give the same results for the same total kick strength. For this excitation range, concentration of the available intensity in a single pulse is preferable. The optimal solution shows a bifurcation at $P \approx 5.0$, after which the optimal alignment improves by splitting the available laser energy into two pulses. Table II shows that the optimized excitation process is very similar to the above described intuitive double-pulse alignment scheme. For $P_t \approx 50$, the double-pulse quantum alignment factor saturates, and the minimal value of $A=0.008$ is reached. However, the optimal solution experiences another branching even before that. At $P_t \approx 11$ a three-pulse solution emerges providing better alignment for the same total kick strength (see Table II). Note that P_1 and P_2 are rather weak compared to the third pulse, and the delay between the first two pulses is $\tau_2 \approx \pi$. Again, the first two pulses create a well prelocalized quantum rotational state that is further squeezed in angle by the third pulse acting as a classical kick. The three-pulse alignment improves with increasing the total kick strength and saturates at $A \approx 0.005$ for $P_t \approx 60$.

TABLE II. Optimal sequence of pulses for a given number (No.) of kicks and for the total kick strength P_t. The table shows the strength of the kicks (P_1, P_2, P_3), the delay time between the kicks (τ_1 and τ_2), the detection time τ_d, and the minimal alignment factor A_{min}.

No.	P_t	P_1	P_2	P_3	τ_1	τ_2	τ_d	A_{min}
1	5	5					2.98	0.088
2	10	4.56	5.65		2.88		0.06	0.034
2	55	4.60	50.4		2.94		0.01	0.008
3	60	4.38	2.88	52.7	2.86	0.13	0.01	0.005

TABLE III. Optimal alignment for a single pulse with finite pulse width σ for a given peak intensity P', and integrated intensity P.

P'	σ	A_{min}	P
200	0.015	0.0866	5.46
400	0.008	0.0851	5.51
800	0.004	0.0844	5.41
1000	0.003	0.0843	5.51
2000	0.002	0.0841	5.51
4000	0.0008	0.0839	6.02
8000	0.0004	0.0839	6.02

C. Alignment with pulses of finite duration

Next, we consider the effect of laser pulses having finite width. We assume that the envelope of the laser pulses has Gaussian shape [see Eq. (23)]. First, we examine the degree of alignment that can be achieved with a single pulse. We are looking for the optimal pulse width σ for a given peak intensity P'. Table III shows the results for different values of P'. It can be seen that the minimal alignment factor decreases with increasing peak intensity. The optimal pulse width decreases too, which is in agreement with the results of Ref. [17]. In order to show that the system approaches the δ-pulse limit for large peak intensities, we calculated the integrated intensity $P=P'\sqrt{\pi}\sigma$ for optimal pulses. It can be seen that for all peak intensities shown in Table III, the integrated intensity is around $P=5.5$, which is close to the first magic strength of a δ pulse [see Fig. 2(a)].

As an example, we consider laser alignment of ICl molecules that have rotational period of $\tau_r=1/(2Bc) \approx 146$ ps. Since the envelope of the laser pulse is $\mathcal{E}^2(t) = 4\pi I_p \exp(-t^2/\Delta_t^2)/c$, where I_p is the peak intensity, the dimensionless peak intensity is related to I_p by

$$P' = \frac{\Delta \alpha I \pi}{\hbar^2 c} I_p . \tag{24}$$

TABLE IV. Optimal alignment with a sequence of two pulses of the duration σ. The optimization is performed for a given value of P_2.

P_2	P_1	σ	τ_1	τ_d	A_{min}
10	4.64	0.007	2.89	0.024	0.022
10	4.63	0.003	2.90	0.036	0.019
20	4.61	0.007	3.02	0.019	0.021
20	4.60	0.003	2.92	0.018	0.011
20	4.60	0.001	2.92	0.022	0.010
30	4.76	0.007	2.98	0.003	0.023
30	4.63	0.003	2.94	0.011	0.011
30	4.60	0.0008	2.93	0.016	0.008

For ICl molecules, $P'=200$ corresponds to $I_p=9.6\times10^{11}$ W/cm^2 and $P'=8000$ corresponds to $I_p=3.8\times10^{13}$ W/cm^2. The pulse duration in Table III ranges from $\Delta_t=350$ fs ($\sigma=0.015$) to $\Delta_t=9$ fs ($\sigma=4\times10^{-4}$).

In order to find the optimal parameters for molecular alignment with two pulses, we minimize the alignment factor for a given (integrated) kick strength P_2 of the second pulse and for different values of the pulse duration. As a starting guess we use the results of optimal double-pulse alignment with δ kicks. The results of the optimization can be seen in Table IV. For a given value of P_2, the degree of alignment can be enhanced by applying shorter pulses (and thus approaching the δ-pulse limit) as in the above described single-pulse case. For very short pulses, the alignment improves with increasing P_2, the same as for δ pulses (Sec. IV B). These results support again our belief that the simplified model of δ kicks (sudden limit) may be rather valuable for identification of the optimal regimes for molecular angular squeezing by a series of short laser pulses. Excitation parameters for ICl for $P_2=10$ and $P_2=30$ are shown in cases (a) and (b) of Table V, respectively. With peak intensities of the order of 10^{12} W/cm^2, enhanced two-pulse alignment should be feasible experimentally.

D. Double-pulse alignment at finite temperature

In the previous sections we investigated the prospects of aligning molecules that are initially in the ground rotational state. Here we analyze the effect of finite temperature on the two-pulse alignment. The quantum-mechanical alignment factor for an ensemble of molecules at temperature T is given by Eq. (15). We calculated the temperature-dependent alignment factor for a quantum rotor having the rotational constant of ICl (Table VI). The excitation parameters are listed in Table V.

TABLE V. Parameters for alignment of ICl molecules with a sequence of two pulses of the duration $\Delta_t=67$ fs. Here, I_{p1} and I_{p2} are the peak intensities of the first and the second pulse, respectively, and τ_1 is the delay time.

	I_{p1} (10^{12} W/cm^2)	I_{p2} (10^{12} W/cm^2)	τ_1 (ps)
(a)	4.1 ($P_1=4.6$)	9.0 ($P_2=10$)	67.5
(b)	4.1 ($P_1=4.6$)	27.0 ($P_2=30$)	68.5
(c)	9.7 ($P_1=10.8$)	27.0 ($P_2=30$)	72.4
(d)	27.0 ($P_1=30$)	27.0 ($P_2=30$)	72.0

TABLE VI. Alignment factor (A_{min}) at different temperatures for the cases (a)–(d) in Table V.

T (K)	(a) A_{min}	(b) A_{min}	(c) A_{min}	(d) A_{min}
0.003	0.019	0.011	0.025	0.066
0.1	0.023	0.014	0.027	0.067
0.3	0.068	0.048	0.049	0.072
8	0.433	0.30	0.175	0.116
33	0.536	0.375	0.318	0.191

Let us consider the example (b). The parameters [case (b) of Table V] are chosen to produce maximal alignment at zero temperature (see Table IV) for the given pulse duration ($\sigma=0.003$ or $\Delta_t=67$ fs). Obviously, the alignment worsens with increasing the temperature. Nevertheless, for low enough temperature ($T<1$ K in our case), a considerable alignment can still be obtained. However, if the thermal rotational energy is of the order of the energy the molecules accumulate during the kick (for ICl molecules and $P_1\approx4.6$ at $T\approx1$ K) the alignment is rather poor. Better alignment at higher temperatures can be obtained by using two relatively strong kicks for excitation. An example can be seen in case (d) of Table VI. Here, the kick strengths are $P_1=P_2=30$ (see Table V). Although excitation with these parameters does not lead to the optimal results at low temperature, it provides enhanced alignment for relatively high temperatures. The pulses needed to obtain a considerable double-pulse alignment at temperature $T\geqslant1$ K are rather intense. In order to avoid ionization of molecules it might be preferable to use more pulses with moderate intensity. As we showed in Ref. [40], applying multiple pulses according to the accumulative squeezing strategy [35] leads to the ''unlimited'' squeezing even at thermal conditions.

V. SUMMARY

In this work we studied the alignment of a molecular system subject to strong, nonresonant laser pulses. The problem was treated as a process of squeezing in the angular coordinate. We analyzed in detail molecular alignment after a single pulse, both in the classical and quantum-mechanical regimes, and defined the limit for single-pulse alignment. Furthermore, we showed that the alignment can be dramatically enhanced by applying a proper sequence of two or more pulses. With the help of quantum control theory, we defined optimal trains of laser pulses leading to effective molecular alignment. According to our estimates, enhanced multipulse molecular alignment is experimentally feasible with the current laser technology. Further analysis of experimental conditions should involve a more elaborated description of molecules, effects of rotational-vibrational coupling, laser noise, spatial inhomogeneity of the laser field, etc. Molecular alignment at these conditions poses new problems,

part of which may be resolved by more sophisticated closed-loop learning control approaches [43,44]. The results of the present paper provide an insight into the physics of multi-pulse alignment, and may serve as an initial guess for more complicated optimization schemes.

ACKNOWLEDGMENT

One of the authors, H.R., acknowledges the support from the National Science Foundation.

APPENDIX A: EXPANSION OF $\exp(iP\cos^2\theta)$ IN SPHERICAL HARMONICS

In this appendix, we calculate the coefficients of the expansion

$$\exp(iP\cos^2\theta)=\sum_{l=0}^{\infty} d_l Y_l^0(\theta). \tag{A1}$$

Due to the parity of the $\cos^2\theta$ interaction, the coefficients d_l are zero for odd l. Therefore, we can write

$$d_{2l}=4\pi\int_0^{\pi/2} d\theta\,\sin\theta\,\exp(iP\,\cos^2\theta)Y_{2l}^0(\theta). \tag{A2}$$

In order to calculate the integral, we express the exponential term as a power series,

$$d_{2l}=4\pi\sum_{\nu=0}^{\infty}\frac{(iP)^\nu}{\nu!}I_{\nu,2l}, \tag{A3}$$

with

$$\begin{aligned} I_{\nu,2l}&=\int_0^{\pi/2} d\theta\sin\theta\cos^{2\nu}\theta\,Y_{2l}^0(\theta)\\ &=\sqrt{\frac{4l+1}{4\pi}}\int_0^{\pi/2} d\theta\,\sin\theta\cos^{2\nu}\theta\,P_{2l}(\cos\theta), \end{aligned} \tag{A4}$$

where P_{2l} are Legendre polynomials. Substituting $x=\cos\theta$, we have

$$I_{\nu,2l}=\sqrt{\frac{4l+1}{4\pi}}\int_0^1 dx\,x^{2\nu}P_{2l}(x), \tag{A5}$$

which is [42]

$$I_{\nu,2l}=\sqrt{\frac{4l+1}{4\pi}}(-1)^l\frac{\Gamma(l-\nu)\Gamma\left(\frac{1}{2}+\nu\right)}{\Gamma(-\nu)\Gamma\left(l+\frac{3}{2}+\nu\right)}. \tag{A6}$$

Note, that the Pochhammer symbol has the value

$$(-\nu)_l=\frac{\Gamma(-\nu+l)}{\Gamma(-\nu)}=0 \quad \text{for } l>\nu, \tag{A7}$$

and therefore $I_{\nu,2l}=0$ for $l>\nu$. The coefficients d_{2l} can now be written as

$$\begin{aligned} d_{2l}&=\sqrt{\pi(4l+1)}(-1)^l\sum_{\nu=l}^{\infty}\frac{(iP)^\nu}{\nu!}(-\nu)_l\frac{\Gamma\left(\nu+\frac{1}{2}\right)}{\Gamma\left(l+\frac{3}{2}+\nu\right)}\\ &=\sqrt{\pi(4l+1)}(-1)^l\sum_{\nu=0}^{\infty}\frac{(iP)^{l+\nu}}{(l+\nu)!}(-\nu-l)_l\\ &\quad\times\frac{\Gamma\left(\nu+l+\frac{1}{2}\right)}{\Gamma\left(2l+\frac{3}{2}+\nu\right)}. \end{aligned} \tag{A8}$$

Next, we express all Gamma functions and factorials in terms of Pochhammer symbols with index ν:

$$\begin{aligned} \Gamma\left(\nu+l+\frac{1}{2}\right)&=\left(l+\frac{1}{2}\right)_\nu\Gamma\left(l+\frac{1}{2}\right),\\ \Gamma\left(2l+\frac{3}{2}+\nu\right)&=\left(2l+\frac{3}{2}\right)_\nu\Gamma\left(2l+\frac{3}{2}\right),\\ (-\nu-l)_l&=(-1)^l(\nu+1)_l=(-1)^l\Gamma(l+1)\frac{(l+1)_\nu}{(1)_\nu},\\ (\nu+l)!&=(l+1)_\nu\Gamma(l+1),\\ \nu!&=(1)_\nu. \end{aligned} \tag{A9}$$

Inserting these relations into Eq. (A8) we get

$$d_{2l}=\sqrt{\pi(4l+1)}(iP)^l\frac{\Gamma\left(l+\frac{1}{2}\right)}{\Gamma\left(2l+\frac{3}{2}\right)}\sum_{\nu=0}^{\infty}\frac{(iP)^\nu}{\nu!}\frac{\left(l+\frac{1}{2}\right)_\nu}{\left(2l+\frac{3}{2}\right)_\nu}. \tag{A10}$$

Now, the sum represents a confluent hypergeometric function, and we can write

$$c_l\equiv d_{2l}=\sqrt{\pi(4l+1)}(iP)^l\frac{\Gamma\left(l+\frac{1}{2}\right)}{\Gamma\left(2l+\frac{3}{2}\right)}{}_1F_1\left(l+\frac{1}{2},2l+\frac{3}{2},iP\right). \tag{A11}$$

APPENDIX B: CLASSICAL ALIGNMENT FACTOR

If the initial temperature of the ensemble of rotors is zero, the classical alignment factor

$$A_{cl}(\tau)=\langle 1-\cos^2\theta\rangle \tag{B1}$$

can be calculated by averaging over the (uniform) initial spatial distribution of the rotors,

$$A_{cl}=1-\frac{1}{2}\int_0^{\pi} d\theta_0 \sin\theta_0 \cos^2[\theta_0-\tau\sin(2\theta)]$$
$$=\frac{1}{2}-\frac{1}{2}\int_0^{\pi/2} d\theta_0 \sin\theta_0 \cos[2\theta_0-2\tau\sin(2\theta_0)]. \quad \text{(B2)}$$

We split the integral into four parts,

$$A_{cl}(\tau)=\frac{1}{2}-\frac{1}{8}\left[\int_0^{\pi} d\theta_0 \sin\left(\frac{3}{2}\theta_0\right)\cos(2\tau\sin\theta_0)\right.$$
$$-\int_0^{\pi} d\theta_0 \sin\left(\frac{1}{2}\theta_0\right)\cos(2\tau\sin\theta_0)$$
$$+\int_0^{\pi} d\theta_0 \cos\left(\frac{1}{2}\theta_0\right)\sin(2\tau\sin\theta_0)$$
$$\left.-\int_0^{\pi} d\theta_0 \cos\left(\frac{3}{2}\theta_0\right)\sin(2\tau\sin\theta_0)\right] \quad \text{(B3)}$$

and with the help of

$$\int_0^{\pi} dx \sin(bx)\cos(a\sin x)=-2b\sin^2\left(\frac{b\pi}{2}\right)s_{-1,b}(a) \quad \text{(B4)}$$

and

$$\int_0^{\pi} dx \cos(bx)\sin(a\sin x)=2\cos^2\left(\frac{b\pi}{2}\right)s_{0,b}(a), \quad \text{(B5)}$$

where

$$s_{\mu,\nu}(z)=\frac{z^{\mu+1}}{(\mu-\nu+1)(\mu+\nu+1)}{}_1\times F_2\left(1;\frac{1}{2}(\mu-\nu+3),\frac{1}{2}(\mu+\nu+3);-\frac{z^2}{4}\right) \quad \text{(B6)}$$

is the Lommel function, we can calculate the integral Eq. (B2) and obtain

$$A_{cl}(\tau)=\frac{1}{2}-\frac{1}{4}\left[\frac{1}{3}{}_1F_2\left(1;\frac{1}{4},\frac{7}{4};-\tau^2\right)-{}_1F_2\left(1;\frac{3}{4},\frac{5}{4};-\tau^2\right)\right]$$
$$-\tau\left[\frac{1}{3}{}_1F_2\left(1;\frac{5}{4},\frac{5}{4};-\tau^2\right)+\frac{1}{5}{}_1F_2\left(1;\frac{3}{4},\frac{9}{4};-\tau^2\right)\right]. \quad \text{(B7)}$$

Finally, we combine the hypergeometric functions to

$$A_{cl}(\tau)=\frac{1}{2}+\frac{1}{6}{}_1F_2\left(1;\frac{7}{4},\frac{5}{4};-\tau^2\right)$$
$$-\frac{8}{15}\tau{}_1F_2\left(2;\frac{7}{4},\frac{9}{4};-\tau^2\right). \quad \text{(B8)}$$

[1] H. Stapelfeldt and T. Seideman, Rev. Mod. Phys. **75**, 543 (2003).
[2] D. Normand, L.A. Lompre, and C. Cornaggia, J. Phys. B **25**, L497 (1992).
[3] P. Dietrich, D.T. Strickland, M. Laberge, and P.B. Corkum, Phys. Rev. A **47**, 2305 (1993).
[4] G.R. Kumar *et al.*, Phys. Rev. A **53**, 3098 (1996).
[5] J.J. Larsen *et al.*, J. Chem. Phys. **111**, 7774 (1999).
[6] B.A. Zon and B.G. Katsnelson, Zh. Eksp. Teor. Fiz. **69**, 1166 (1975) [Sov. Phys. JETP **42**, 595 (1976)].
[7] B. Friedrich and D. Herschbach, Phys. Rev. Lett. **74**, 4623 (1995); J. Phys. Chem. **99**, 15 686 (1995).
[8] W. Kim and P.M. Felker, J. Chem. Phys. **104**, 1147 (1996).
[9] C.H. Lin, J.P. Heritage, and T.K. Gustafson, Appl. Phys. Lett. **19**, 397 (1971); J.P. Heritage, T.K. Gustafson, and C.H. Lin, Phys. Rev. Lett. **34**, 1299 (1975).
[10] A.D. Bandrauk and L. Claveau, J. Phys. Chem. **93**, 107 (1989).
[11] P.M. Felker, J. Phys. Chem. **96**, 7844 (1992).
[12] T. Seideman, J. Chem. Phys. **103**, 7887 (1995); **106**, 2881 (1997).
[13] T. Seideman, Phys. Rev. Lett. **83**, 4971 (1999).
[14] J. Ortigoso, M. Rodrigues, M. Gupta, and B. Friedrich, J. Chem. Phys. **110**, 3870 (1999).
[15] B.A. Zon, Eur. Phys. J. D **8**, 377 (2000).
[16] L. Cai, J. Marango, and B. Friedrich, Phys. Rev. Lett. **86**, 775 (2001).
[17] F. Rosca-Pruna and M.J.J. Vrakking, Phys. Rev. Lett. **87**, 153902 (2002); J. Chem. Phys. **116**, 6567 (2002); **116**, 6579 (2002).
[18] I.V. Litvinyuk, K.F. Lee, P.W. Dooley, D.M. Rayner, D.M. Villeneuve, and P.B. Corkum, Phys. Rev. Lett. **90**, 233003 (2003).
[19] P.W. Dooley, I.V. Litvinyuk, K.F. Lee, D.M. Rayner, M. Spanner, D.M. Villeneuve, and P.B. Corkum, Phys. Rev. A **68**, 023406 (2003).
[20] V. Renard, M. Renard, S. Guerin, Y.T. Pashayan, B. Lavorel, O. Faucher, and H.R. Jauslin, Phys. Rev. Lett. **90**, 153601 (2003).
[21] E. Peronne, M.D. Poulsen, C.Z. Bisgaard, H. Stapelfeldt, and T. Seideman, Phys. Rev. Lett. **91**, 043003 (2003).
[22] M. Machholm and N.E. Henriksen, Phys. Rev. Lett. **87**, 193001 (2001).
[23] M. Machholm, J. Chem. Phys. **115**, 10 724 (2001).
[24] D.M. Villeneuve, S.A. Aseyev, A. Avery, and P.B. Corkum, Appl. Phys. B: Lasers Opt. **74**, S157 (2002).
[25] J.G. Underwood, M. Spanner, M.Yu. Ivanov, J. Mottershead, B.J. Sussman, and A. Stolow, Phys. Rev. Lett. **90**, 223001 (2003).
[26] R.A. Bartels *et al.*, Phys. Rev. Lett. **88**, 013903 (2002).
[27] V. Kalosha *et al.*, Phys. Rev. Lett. **88**, 103901 (2002).
[28] R. Velotta *et al.*, Phys. Rev. Lett. **87**, 183901 (2001).
[29] M. Leibscher, I.Sh. Averbukh, and H. Rabitz, Phys. Rev. Lett. **90**, 213001 (2003).

[30] R.S. Judson, K.K. Lehmann, H. Rabitz, and W.S. Warren, J. Mol. Spectrosc. **223**, 425 (1990).
[31] L.Y. Shen, and H. Rabitz, J. Phys. Chem. **95**, 1047 (1991).
[32] J. Ortigoso, Phys. Rev. A **57**, 4592 (1998).
[33] K. Hoki and Y. Fujimura, Chem. Phys. **267**, 187 (2001).
[34] C.M. Dion, A. Ben Haj-Yedder, E. Cancés, C. Le Bris, A. Keller, and O. Atabek, Phys. Rev. A **65**, 063408 (2002).
[35] I.Sh. Averbukh and R. Arvieu, Phys. Rev. Lett. **87**, 163601 (2001).
[36] M. Leibscher and I.Sh. Averbukh, Phys. Rev. A **65**, 053816 (2002).
[37] W.H. Oskay, D.A. Steck, and M.G. Raizen, Phys. Rev. Lett. **28**, 283001 (2002).
[38] I.Sh. Averbukh, R. Arvieu, and M. Leibscher, in *Coherence and Quantum Optics VIII*, edited by N.P. Bigelow, J.H. Eberly, C.R. Stroud, Jr., and I.A. Walmsley (Kluwer Academic/Plenum, New York, 2003), pp. 71–86.
[39] R.W. Boyd, *Nonlinear Optics* (Academic Press, Boston, 1992).
[40] M. Leibscher, I. Sh. Averbukh, P. Rozmej, and R. Arvieu, Phys. Rev. A (to be published); e-print quant-ph/0306146.
[41] B. Friedrich and D. Herschbach, J. Phys. Chem. A **103**, 10 280 (1999).
[42] I.S. Gradshtein, *Table of Integrals, Series and Products* (Academic Press, San Diego, 2000).
[43] R.S. Judson and H. Rabitz, Phys. Rev. Lett. **68**, 1500 (1992).
[44] T.C. Weinacht and P. Bucksbaum, J. Opt. B: Quantum Semiclassical Opt. **4**, R35 (2002).